Research Article

Open Access

Effect of a time dependent stenosis on flow of a second order fluid through constricted tube with velocity slip at wall using integral method

Abstract

The effect of time dependent, axially symmetric constriction in a tube of constant cross section, through which a non-Newtonian fluid is flowing steadily; is modeled and the analysis was made using integral approach. The present article is stationed on second order fluid model. The study is made applicable for mild constriction by using an order of magnitude analysis. The effect of different parameters, non-Newtonian characteristics, Reynolds number and time looming in the model on velocity distribution, wall shear stress, separation and reattachment and pressure gradient are reviewed graphically. It is observed that Reynolds number gives a mechanism to oversight the attachment and de-attachment data. Constricted tube Non-Newtonian fluids Time dependent stenosis Slip velocity Shear stress.

Keywords: integral method, non-Newtonian fluid, Reynolds number, viscometric flows, Rivlin-Ericksen tensors, Karman-Pohlhausen method

Volume 2 Issue 3 - 2018

NZ Khan,[1] MA Rana,[1] AM Siddiqui[2]

[1]Riphah International University, Pakistan
[2]Pennsylvania State University, York campus, USA

Correspondence: Nosheen Zareen Khan, Assistant Professor, Ripah International University, Islamabad, Pakistan, Tel +923325549737, Email noshikhan14@yahoo.com

Received: April 30, 2018 | **Published:** June 05, 2018

Introduction

Constriction is the development of arteriosclerotic plaques in the luman of an artery which produce major circulatory derangement.[1–3] Fluid dynamic characteristics of blood flow are the curtain-raiser to understand and diagnosis the diseases and their treatment.[4–9] Blood flow model through constricted tubes are analyzed by many researchers.[10–17]

The experimental studies on the steady and unsteady fluid flow through constricted channels are reported by DF Young et al.[4,18] The fluid flow through infected artery is considered theoretically.[15] At less shear rate blood is treated as Newtonian fluid.[19] Non-Newtonian and steady blood flow through sicked artery is presented by D Biswas[20] analytically and by SR Verma[21] numerically studies the fluid flow through tepid obstructed tube analytically. Few studies considered the no slip property at uniform and constricted walls.[11–15] A Mirza et al.,[22] discussed the steady, non-Newtonian and incompressible fluid flowing through constricted artery. AM Siddiqui et al.,[23] has discussed the blood flow through tepid obstructed artery where the slip is neglected and analytic technique is used to find the solution by considering the constant volume flow rate. In the above mentioned research papers the usual time independent constriction has been taken. Experimental observations[24,25] and theoretical observations[26–28] on blood flow reveals that there exist slip velocity at boundary. P Brunn[29] has analyzed the velocity slip at the boundaries analytically and compared the result with the experimental data of five different viscometric flows. JC Misra et al.,[30] developed a mathematical model to study the blood flow characteristic through constricted vessels by considering the slip velocity at wall of the vessels. D Biswas[20] studied the effect of slip on velocity side view, pressure drop and wall shear. Different stages of constriction such as mild, moderate and sever for non-Newtonian fluids with slip property are presented by JC Misra et al.,[31] The developments in non-Newtonian fluids is contributed by many authors studied the non-Newtonian Bingham plastic blood flow through the constricted artery with slip velocity at wall and solved the non-linear differential equation analytically.[32–35] A Bhatnagar et al.,[36] reported the effect of slip velocity on non-Newtonian (Herschel-Bulkely) fluid flow through constricted artery. They derived the non-dimensional results for skin friction, flow resistance, flow rate and axial velocity. NZ khan et al.,[37] extended the work of JH Forrester et al.,[38] for second order fluid through constricted tube with slip velocity at wall. DF Young[10] & PN Tandon[39] considered the time rate of change of radius. The aim of this work is to study the effect of time dependent constriction with slip effects at wall for second order fluid flow.

Governing equations

The governing equations for an incompressible fluid, where body forces are neglected, given as[40]

$$\nabla.\tilde{\mathbf{V}} = 0, \tag{1}$$

$$\rho\left(\frac{\tilde{\nabla}(\tilde{\mathbf{V}})^2}{2} - \tilde{\mathbf{V}}\times(\tilde{\nabla}\times\tilde{\mathbf{V}})\right) = -\tilde{\nabla}p + (\alpha_1+\alpha_2)\nabla.\tilde{A}_1^2 + \mu\tilde{\nabla}.\tilde{A}_1 + \alpha_1((\tilde{\mathbf{V}}.\tilde{\nabla})\tilde{\nabla}.\tilde{A}_1 + (\tilde{\nabla}\tilde{\mathbf{V}})^T\tilde{\nabla}.\tilde{A}_1 + \tilde{A}_1.\tilde{\nabla}(\tilde{\nabla}\tilde{\mathbf{V}})^T), \tag{2}$$

where $\tilde{\mathbf{V}}, \rho, \mu, \alpha_1, \alpha_2, \tilde{\mathbf{A}}_1$ *and* $\tilde{\mathbf{A}}_2$ are the velocity vector, constant density, dynamic viscosity, material constants, first and second Rivlin-Ericksen tensors. The Rivlin-Ericksen tensors are exemplify as

$$\tilde{\mathbf{A}}_1 = \left(\tilde{\nabla}\tilde{\mathbf{V}}\right)^T + \tilde{\nabla}\tilde{\mathbf{V}}, \tag{3}$$

And

$$\tilde{\mathbf{A}}_2 = \frac{d\tilde{\mathbf{A}}_1}{dt} + \left(\tilde{\mathbf{A}}_1\left(\tilde{\nabla}\tilde{\mathbf{V}}\right)\right)^T + \tilde{\mathbf{A}}_1\left(\tilde{\nabla}\tilde{\mathbf{V}}\right). \tag{4}$$

For the model (2) the material constraints are defined as[41]

$$\alpha_1 \le 0, \mu \ge 0, \text{and}\,\alpha_1 + \alpha_2 \ge 0. \tag{5}$$

Problem formulation

A steady, laminar and incompressible flow of a second order fluid through constricted tube having transient cosine framed symmetric constriction of height δ is considered. R_0, $\tilde{R}(\tilde{z})$ are the radii of the normal and constricted tube. The $\tilde{z}-$ and $r-$axis are taken along the flow direction and normal to it and t is time. Following the tube boundary is defined as[10]

$$\tilde{R}(\tilde{z}) = \begin{cases} R_0 - \dfrac{\delta}{2}(1-e^{-t/T})(1+\cos(\dfrac{\pi \tilde{z}}{z_0})), & -z_0 < \tilde{z} < z_0 \\ R_0. & otherwise \end{cases} \tag{6}$$

In Eq. (6), T is the time constant and z_0 is the length of the constricted part as shown in the Figure 1. Radius of normal tube can be obtained by taking $t = 0$.

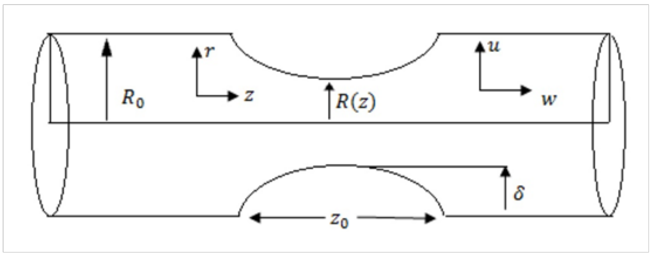

Figure 1 Geometry of the problem.

The velocity vector $\tilde{\mathbf{V}}$ for axisymmetric and time independent is taken of the form

$$\tilde{\mathbf{V}} = \left[\tilde{u}\left(\tilde{r},\tilde{z}\right), 0, \tilde{w}\left(\tilde{r},\tilde{z}\right)\right]. \tag{7}$$

Where $\tilde{u}$ and $\tilde{w}$ are the velocity components in $\tilde{r}-$, $\tilde{z}-$ directions respectively. According to the geometry of the problem the boundary conditions are

$$\tilde{u} = \tilde{w} = v_s \text{ at } \tilde{r} = R\left(\tilde{z}\right), \frac{\partial \tilde{w}}{\partial \tilde{r}} = 0 \text{ at } \tilde{r} = 0. \tag{8}$$

In view of Eq. (8) the Eqs. (1) and (2) become

$$\frac{\partial \tilde{u}}{\partial \tilde{r}} + \frac{\partial \tilde{w}}{\partial \tilde{z}} + \frac{\tilde{u}}{\tilde{r}} = 0, \tag{9}$$

$$\frac{\partial \tilde{h}}{\partial \tilde{r}} - \rho\tilde{w}\Omega = -\mu\frac{\partial \Omega}{\partial \tilde{z}} - \alpha_1\tilde{w}(\nabla^2\Omega - \frac{\Omega}{\tilde{r}^2}) + (\alpha_1+\alpha_2)(\frac{2}{\tilde{r}}\frac{\partial(\tilde{u}\Omega)}{\partial \tilde{z}}), \tag{10}$$

$$\frac{\partial \tilde{h}}{\partial \tilde{z}} + \rho\tilde{u}\Omega = \mu(\frac{\partial \Omega}{\partial \tilde{r}} + \frac{\Omega}{\tilde{r}}) + \alpha_1\tilde{u}(\nabla^2\Omega - \frac{\Omega}{\tilde{r}^2}) - (\alpha_1+\alpha_2)(\frac{2}{\tilde{r}}\frac{\partial(\tilde{u}\Omega)}{\partial \tilde{r}}), \tag{11}$$

Where

$$\Omega = \frac{\partial \tilde{w}}{\partial \tilde{r}} - \frac{\partial \tilde{u}}{\partial \tilde{z}}, \tag{12}$$

$$\tilde{h} = \frac{\rho}{2}\left(\tilde{u}^2+\tilde{w}^2\right) - \alpha_1\left(\tilde{u}\nabla^2\left(\tilde{u} - \frac{\tilde{u}}{\tilde{r}^2}\right) + \tilde{w}\nabla^2\tilde{w}\right) - \frac{1}{4}(3\alpha_1+2\alpha_2)\left|\tilde{\mathbf{A}}_1\right|^2 + p, \tag{13}$$

$$|\tilde{\mathbf{A}}_1|^2 = 4(\frac{\partial \tilde{u}}{\partial \tilde{r}})^2 + 4(\frac{\partial \tilde{w}}{\partial \tilde{z}})^2 + 4(\frac{\tilde{u}}{\tilde{r}})^2 + 2(\frac{\partial \tilde{w}}{\partial \tilde{r}} + \frac{\partial \tilde{u}}{\partial \tilde{z}})^2, \tag{14}$$

and the Laplacian, generalized pressure are expressed as ∇^2 and $\tilde{h}$. Introducing the dimensionless variables

$$r = \frac{\tilde{r}}{R_0}, z = \frac{\tilde{z}}{z_0}, w = \frac{\tilde{w}}{U_0}, u = \frac{\tilde{u}z_0}{U_0\delta}, h = \frac{\tilde{h}}{\rho U_0^2}, p = \frac{\tilde{p}}{\rho U_0^2}, R_e = \frac{U_0 R_0 \rho}{\mu}, \tag{15}$$

where U_0 is the average velocity. Order-of-magnitude reasoning is used to determine the imperceptible effects which are given in Eqs. (9) -(14). Now Eq. (9) becomes

$$\frac{\partial w}{\partial z} + \frac{\delta}{R_0}\frac{1}{r}\frac{\partial u}{\partial r} = 0. \tag{16}$$

From Eq. (15) using order of magnitude technique, which is also suitable for non-Newtonian fluids[10], it is notable that $\frac{1}{R_e}\frac{\delta}{R_0} \ll 1$, $u \ll w$, $\frac{\delta}{z_0} \ll 1$, $\frac{R_0}{z_0} \sim O(1)$ then normal axial stress component $\frac{\partial^2 w}{\partial z^2}$ is imperceptible as compared to the gradient of shear. So Eqs. (9) and (13) becomes

$$\frac{\partial h}{\partial r} = 0. \tag{17}$$

$$\frac{\partial h}{\partial z} = \frac{1}{R_e}\left[\frac{\partial^2 w}{\partial r^2} + \frac{1}{r}\frac{\partial w}{\partial r}\right], \tag{18}$$

$$h = \frac{w^2}{2} - \alpha^* w\left(\frac{\partial^2 w}{\partial r^2} + \frac{1}{r}\frac{\partial w}{\partial r}\right) - \alpha^*\frac{1}{2}\left(\frac{\partial w}{\partial r}\right)^2 - \beta^*\left(\frac{\partial w}{\partial r}\right)^2 + p. \tag{19}$$

where $\alpha^* = \frac{\alpha_1}{R_0^2\rho}$ and $\beta^* = \frac{\alpha_1+\alpha_2}{R_0^2\rho}$. The non-dimensional form of time dependent cosine shape obstruction profile is

$$R(z) = \begin{cases} 1 - \dfrac{\delta^*}{2}(1-e^{-t^*})(1+\cos(\pi z)), & -1 < z < 1 \\ 1. & otherwise \end{cases} \tag{20}$$

where $\delta^* = \delta / R_0$ and $t^* = t/T$. Eq. (18) can be integrated from $r = 0$ to $r = R$ to get

$$\int_0^R r\frac{\partial h}{\partial z}dr = \frac{R}{R_e}\left(\frac{\partial w}{\partial r}\right)_R. \tag{21}$$

Exact solution of Eq. 21 is not possible. We can find the approximate solution by assuming fourth order polynomial which is called Karman-Pohlhausen method.[42] Therefore

$$\frac{w}{U} = A_1 + A_2\left(1-\frac{r}{R}\right) + A_3\left(1-\frac{r}{R}\right)^2 + A_4\left(1-\frac{r}{R}\right)^3 + A_5\left(1-\frac{r}{R}\right)^4, \quad (22)$$

Where U is the centerline velocity and $A_1, A_2, A_3, A_4 and A_5$ are the unknown coefficients which can be found by using the five conditions given below

$$w = v_S \text{ at } r = R, \quad (23)$$

$$w = U \text{ at } r = 0, \quad (24)$$

$$\frac{\partial w}{\partial r} = 0 \text{ at } r = 0, \quad (25)$$

$$\frac{dh}{dz} = \frac{1}{R_e}\left(\frac{\partial^2 w}{\partial r^2} + \frac{1}{r}\frac{\partial w}{\partial r}\right) \text{ at } r = R, \quad (26)$$

$$\frac{\partial^2 w}{\partial r^2} = -2\frac{U}{R^2} \quad \text{at } r = 0. \quad (27)$$

The velocity slip at the boundary and centerline velocity U is defined by Eqs. (23) and (24) condition (24) is a simple definition, (26) is attained from equation (18). The assumption for the velocity of the fluid is parabolic can be expressed as $\left(w = U\left[1-\frac{r^2}{R^2}\right]\right)$ at the center (r=0) of the tube, so that the second derivative of w with respect to r, we get the condition (26). Thus Eq. (22) becomes

$$\frac{w}{U} = \left(-\lambda + 10 - 12\frac{v_s}{U}\right)\frac{\eta}{7} + \left(3\lambda + 5 - 6\frac{v_s}{U}\right)\frac{\eta^2}{7} + \left(-3\lambda - 12 + 20\frac{v_s}{U}\right)\frac{\eta^3}{7} + \left(\lambda + 4 - 9\frac{v_s}{U}\right)\frac{\eta^4}{7} + \frac{v_s}{U}, \quad (28)$$

Where

$$\lambda = \frac{R^2 R_e}{U}\frac{dh}{dz}. \quad (29)$$

and $\eta = \left(1-\frac{r}{R}\right)$. It is notable that λ is dependent only on z, since R, U and h are function of z. In Eq. (29) U and h are undetermined. The flux Q through the tube is defined as

$$Q = \int_0^R 2\pi r w dr. \quad (30)$$

Using Eq. (28) in (30) we obtain

$$Q = \frac{\pi R^2 U}{210}\left(-2\lambda U + 97U + 51v_s\right), \quad (31)$$

And centerline velocity U is defined as

$$U = \frac{210}{97}.\frac{1}{\pi R^2}\left[Q + \frac{\pi R^4 R_e}{105}\frac{dh}{dz} - \frac{17}{70}v_s \pi R^2\right]. \quad (32)$$

Using Eq. (19) in (21) to get

$$\frac{1}{2}\frac{d}{dz}\int_0^R r w^2 dr - \alpha^*\frac{d}{dz}\left(R v_s\left(\frac{\partial w}{\partial r}\right)_R - \frac{1}{2}\int_0^R r\left(\frac{\partial w}{\partial r}\right)^2 dr\right) - \beta^*\frac{d}{dz}\int_0^R r\left(\frac{\partial w}{\partial r}\right)^2 dr + \frac{R^2}{2}\frac{dP}{dz} = \frac{1}{R_e}\left(\frac{\partial w}{\partial r}\right)_R, \quad (33)$$

And in order to get closed form of solution it is assumed that velocity profile is parabolic, i.e

$$w = U\left[1-\frac{r^2}{R^2}\right], \quad (34)$$

As discussed by JH Forrester et al.,[38] if we neglect the non-linear terms the flow through obstruction becomes Poiseuille. Substitution of Eqs. (34) and (29) into Eq. (19) and (33) yields generalized pressure and pressure gradient

$$\frac{dh}{dz} = 48\alpha^*\frac{Q^2}{\pi^2}\frac{1}{R^7}\frac{dR}{dz} - 28\alpha^* v_s\frac{Q^2}{\pi^2}\frac{1}{R^5}\frac{dR}{dz} + 24\beta^*\frac{Q^2}{\pi^2}\frac{1}{R^7}\frac{dR}{dz} + \frac{dp}{dz}, \quad (35)$$

$$\frac{dp}{dz} = \frac{388}{225}\frac{1}{R^5}\frac{Q}{\pi}\frac{dR}{dz} - \frac{8}{R^4 R_e} + \frac{2608}{75}\frac{Q^2}{\pi^2}\frac{\alpha^*}{R^7}\frac{dR}{dz} + \frac{5216}{75}\frac{Q^2}{\pi^2}\frac{\beta^*}{R^7}\frac{dR}{dz} + \frac{v_s}{25}\left(\frac{\alpha^*}{R^5}\frac{Q^2}{\pi^2}\frac{dR}{dz} + \frac{Q^2}{\pi^2}\frac{436}{R^2 R_e}\right). \quad (36)$$

In order to get velocity w, we put Eqs. (32) and (33) in Eq. (29) and (28) to get

$$w = \frac{2}{R^2}\frac{Q}{\pi}\left[2\eta - \eta^2\right] + \frac{1}{R^3}\frac{dR}{dz}\left[-11\eta + 43\eta^2 - 45\eta^3 + 15\eta^4\right]$$
$$\left[\frac{4}{225}R_e\frac{Q}{\pi}\frac{dR}{dz} - \frac{4}{25}R_e\alpha^* v_s\frac{Q^2}{\pi^2} + \frac{64}{75}R_e\frac{\alpha^*}{R^2}\frac{Q^2}{\pi^2} + \frac{128}{75}\beta^*\frac{R_e}{R^2}\frac{Q^2}{\pi^2}\right]$$
$$+v_s\left[1 - \frac{1}{16975}(75422\eta - 110311\eta^2 + 73540\eta^3 - 18855\eta^4)\right], \quad (37)$$

where $\eta = 1 - r/R$, . Velocity for normal tube can be obtained by substituting t^*=0 . The volume flow flux in normal tube is $\tilde{Q} = \pi R_0^2 U_0$, which gives non-dimensional flux $Q = \tilde{Q}/R_0^2 U_0 = \pi$ which is same for obstructed tube.[43–44] So the expressions for the velocity w and pressure gradient $\frac{dP}{dz}$ becomes

$$w = \frac{2}{R^2}[2\eta - \eta^2] + \frac{1}{R^3}\frac{dR}{dz}[-11\eta + 43\eta^2 - 45\eta^3 + 15\eta^4]$$
$$\left[\frac{4}{225}R_e\frac{dR}{dz} - \frac{4}{25}R_e\alpha^* v_s + \frac{64}{75}R_e\frac{\alpha^*}{R^2} + \frac{128}{75}\beta^*\frac{R_e}{R^2}\right]$$
$$+v_s[1 - \frac{1}{16975}\left(75422\eta - 110311\eta^2 + 73540\eta^3 - 18855\eta^4)\right], \quad (38)$$

Citation: Khan NZ, Rana MA, Siddiqui AM. Effect of a time dependent stenosis on flow of a second order fluid through constricted tube with velocity slip at wall using integral method. *Fluid Mech Res Int.* 2018;2(3):118–126. DOI: 10.15406/fmrij.2018.02.00027

$$\frac{dp}{dz}=\frac{388}{225}\frac{1}{R^5}\frac{dR}{dz}-\frac{8}{R^4R_e}+\frac{2608}{75}\frac{\alpha^*}{R^7}\frac{dR}{dz}+\frac{5216}{75}\frac{\beta^*}{R^7}\frac{dR}{dz}+\frac{v_s}{25}\left(\frac{\alpha^*}{R^5}\frac{dR}{dz}+\frac{436}{R^2R_e}\right). \tag{39}$$

As a special case the velocity profile[10] can be obtain by taking

$\alpha^*=\beta^*=0$ in Eq. (38).

Pressure distribution

Pressure distribution at any sector z along the constriction can be obtained when Eq. (39) is integrated using boundary condition that is $p=p_0$ at $z=z_0$.

$$(\Delta p)=\frac{388}{225}\int_{R_0}^{R}\frac{1}{R^5}dR+\frac{v_s}{25}\alpha^*\int_{R_0}^{R}\frac{1}{R^5}dR+\left(\frac{2608}{75}\alpha^*+\frac{5216}{75}\beta^*\right)\int_{R_0}^{R}\frac{1}{R^7}dR+\frac{v_s}{R_e}\frac{z_0}{R_0^2}\int_{z_0}^{z}\frac{1}{R^2}dz-\frac{8}{R_e}\int_{z_0}^{z}\frac{1}{R^4}dz, \tag{40}$$

or

$$(\Delta p)=\left(\frac{78}{25}v_s\alpha^*+\frac{97}{225}\right)\left(\frac{1}{R^4}-\frac{1}{R_0^4}\right)\left(\frac{1304}{225}\alpha^*+\frac{2608}{225}\beta^*\right)\left(\frac{1}{R^6}-\frac{1}{R_0^4}\right)-\frac{v_s}{R_e}\frac{z_0}{\pi R_0^2}\int_{z_0}^{z}\frac{1}{[a-b\cos u]^2}dz-\frac{8}{\pi R_e}\frac{z_0}{\pi R_0^4}\int_{z_0}^{z}\frac{1}{[a-b\cos u]^4}dz, \tag{41}$$

Where

$$a=1-\frac{\delta^*}{2},\; b=\frac{\delta^*}{2}. \tag{42}$$

Now

$$\int_0^{\pi}\frac{1}{a-b\cos u}du=\pi\left(a^2-b^2\right)^{-1/2}. \tag{43}$$

Differentiating Eq. (43) partially with respect to *a,* we get

$$\int_0^{\pi}\frac{1}{[a-b\cos u]^2}du=\pi a(a^2-b^2)^{-3/2}=\pi g\left(\frac{\delta}{R_0}\right), \tag{44}$$

$$\int_0^{\pi}\frac{1}{[a-b\cos u]^4}du=\pi a\left(a^2+\frac{3}{2}b^2\right)(a^2-b^2)^{-7/2}=\pi f\left(\frac{\delta}{R_0}\right), \tag{45}$$

Where

$$g(\delta^*)=\left(1-\frac{\delta^*}{2}\right)(1-\delta^*)^{-3/2}, \tag{46}$$

$$f(\delta^*)=\left(1-\frac{\delta^*}{2}\right)\left(1-\delta^*+\frac{5}{8}(\delta^*)^2\right)(1-\delta^*)^{-7/2}, \tag{47}$$

So that

$$(\Delta p)=\left(\frac{78}{25}v_s\alpha^*+\frac{97}{225}\right)\left(\frac{1}{R^4}-\frac{1}{R_0^4}\right)-\frac{8}{\pi R_e}\frac{z_0}{R_0^4}f(\delta^*)\left(\frac{1304}{225}\alpha^*+\frac{2608}{225}\beta^*\right)\left(\frac{1}{R^6}-\frac{1}{R_0^6}\right)+\frac{v_s}{R_e}\frac{z_0}{R_0^2}g(\delta^*). \tag{48}$$

For normal tube i-e $t=0$ or $\delta=0$ and $f\left(\frac{\delta}{R_0}\right)=g\left(\frac{\delta}{R_0}\right)=1,$ the pressure distribution is given by

$$\left(\Delta p\right)_P=-\frac{16z_0}{R_eR_0^4}+\frac{v_s}{R_e}\frac{z_0}{R_0^2}. \tag{49}$$

In unobstructed tube the Poiseuille flow is defined by subscript P. If tube length is $2L$, then the pressure across the whole length of the constricted artery can be expressed as

$$[\Delta p]=\left(\frac{78}{25}v_s\alpha^*+\frac{97}{225}\right)\left(\frac{1}{R^4}-\frac{1}{R_0^4}\right)\left(\frac{1304}{225}\alpha^*+\frac{2608}{225}\beta^*\right)\left(\frac{1}{R^6}-\frac{1}{R_0^6}\right)+\frac{8}{\pi R_e}\frac{(2L-2z_0)}{R_0^4}f(\delta^*)-\frac{v_s}{R_e}\frac{(2L-2z_0)}{R_0^2}g(\delta^*). \tag{50}$$

For normal tube, $z_0=0$ the expression for the pressure distribution will become

$$\left[\Delta p\right]_P=\frac{8}{\pi R_e}\frac{2L}{R_0^4}f(\delta^*)-\frac{v_S}{R_e}\frac{2L}{R_0^2}g(\delta^*). \tag{51}$$

We note that Eqs. (48) and (50) carry the results of (10) as a special case for $\alpha^*=\beta^*=0.$

Shear Stress on Constricted Surface

The shear stress on the obstructed surface is

$$\tau_{\tilde{w}}=-\left(\mu\left(\frac{\partial\tilde{w}}{\partial\tilde{r}}+\frac{\partial\tilde{u}}{\partial\tilde{z}}\right)-\alpha_2\left[\frac{\tilde{u}}{\tilde{r}^2}\left(\frac{\partial\tilde{w}}{\partial\tilde{r}}+\frac{\partial\tilde{u}}{\partial\tilde{z}}\right)\right]\right)_R-\left(\alpha_1\left[\left(\tilde{u}\frac{\partial}{\partial\tilde{r}}+\tilde{w}\frac{\partial}{\partial\tilde{z}}\right)\left(\frac{\partial\tilde{u}}{\partial\tilde{z}}+\frac{\partial\tilde{w}}{\partial\tilde{r}}\right)+2\frac{\partial\tilde{u}}{\partial\tilde{r}}\frac{\partial\tilde{u}}{\partial\tilde{z}}+2\frac{\partial\tilde{w}}{\partial\tilde{r}}\frac{\partial\tilde{w}}{\partial\tilde{z}}\right]\right)_R \tag{52}$$

The shear stress can be found by substituting Eq. (15) in Eq. (52), i.e

$$\frac{\tau_{\tilde{w}}}{\rho U_0^2}=\frac{-1}{R_e}\left(\frac{\partial w}{\partial r}\right)_R-\alpha^*\left(\frac{\partial w}{\partial r}\frac{\partial w}{\partial z}\right)_R. \tag{53}$$

From Eq. (38) and (53), we obtain

$$\tau_W = \left[\frac{4}{R^3} - \frac{44}{25}\frac{1}{R^4}\frac{dR}{dz}\left(\frac{R_e}{9} - R_e v_s \alpha^* + \frac{16}{3}R_e\frac{\alpha^*}{R^3} + \frac{32}{3}R_e\frac{\beta^*}{R^3}\right) + \frac{75422}{16975}\frac{v_s}{R}\right]$$
$$\left[-\frac{1}{R_e} - \alpha^*\frac{dR}{dz}\left(-\frac{4}{R^3} + \frac{44}{25}\frac{1}{R^4}\frac{dR}{dz}\left(\frac{R_e}{9} - R_e v_s \alpha^* + \frac{16}{3}R_e\frac{\alpha^*}{R^*} + \frac{32}{3}R_e\frac{\beta^*}{R^3}\right) + \frac{75422}{16975}\frac{v_s}{R}\right)\right]. \quad (54)$$

For $\alpha^* = \beta^* = 0$, the results of (10) can be found. Shear Stress in unobstructed tube will be

$$\left(\tau_w\right)_p = \frac{4}{R^3 R_e} + \frac{75422}{16975}\frac{v_S}{R_e R}. \quad (55)$$

Separation and reattachment

The separation and reattachment data can be found by taking imperceptible effects of shear stress at the wall,[42] i.e $\tau_w = 0$.

$$\left[\frac{4}{R^3} + \frac{R_e}{R^5}\frac{dR}{dz}\left(\frac{528}{97}\alpha^* - \frac{19344}{16975}v_s\alpha^* R^2 - \frac{44}{225}R^2\right)\right]$$
$$\left[\frac{1}{R_e} + \alpha^*\frac{dR}{dz}\left(\frac{4}{R^3} + \frac{R_e}{R^5}\frac{dR}{dz}\left(\frac{528}{97}\alpha^* - \frac{19344}{16975}v_s\alpha^* R^2 - \frac{44}{225}R^2\right)\right)\right] = 0, \quad (56)$$

$$R_e = \frac{A}{4938\frac{dR}{dz}B}, \frac{C \pm \sqrt{C^2 - 1.82572236\times 10^{10} B}}{59752\left(\frac{dR}{dz}\right)^2 B}, \quad (57)$$

Where

$$A = 9\left(33950R^4 - 37711R^6 v_S + 14938\frac{dR}{dz}R^3 v - s\alpha^*\right),$$

$$B = R^3 + 48\alpha^* + 96\beta^*, C = 611100\frac{dR}{dz}R^4\alpha^* - 678798\frac{dR}{dz}R^6 v_s\alpha^* + 268884\left(\frac{dR}{dz}\right)^2 R^3 v_s\alpha^*.$$

(58)Results and discussion

In this theoretical study the blood is considered as second order two-dimensional fluid flowing in a constricted tube of infinite length. The results are applicable on mild constriction.

In (Figures 2) (Figure 3) the change of non-Newtonian parameter α^* and β^* on the non dimensional velocity profile with and without slip is depicted at $z = 0.475$ taking $R_e = 5$, $\delta^* = 0.083$, $t^* = 3$.

It is notable that velocity increases with an increase in non-Newtonian characteristic (with and without slip) which is true in physical phenomena. On the other hand non dimensional velocity increases with slip effects. It is evident from Figure 4 that when Reynolds number boost velocity of the fluid also rise near the throat of the constriction, however, it decline in the diverging region, physically it means that viscous forces are dement over the inertia forces. Effect of Reynolds number for Newtonian fluids can be examined in Figure 5.[10]

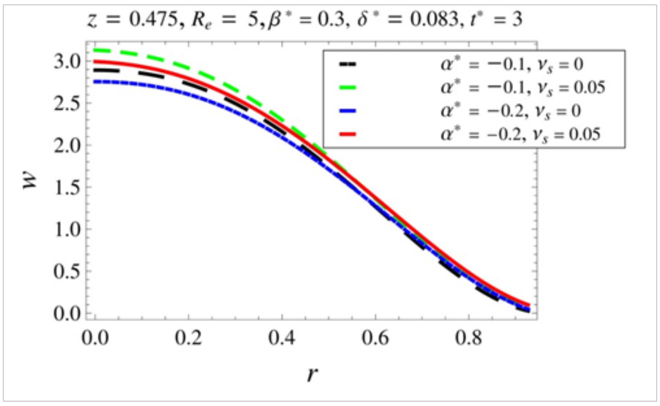

Figure 2 Effect of non-Newtonian parameter α^* on velocity profile.

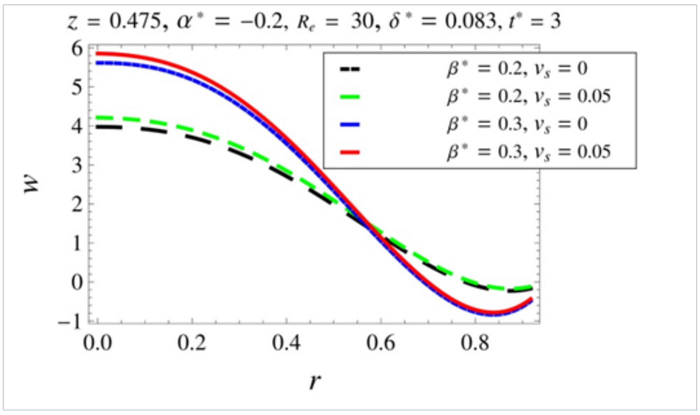

Figure 3 Effect of non-Newtonian characteristic β^* on velocity profile.

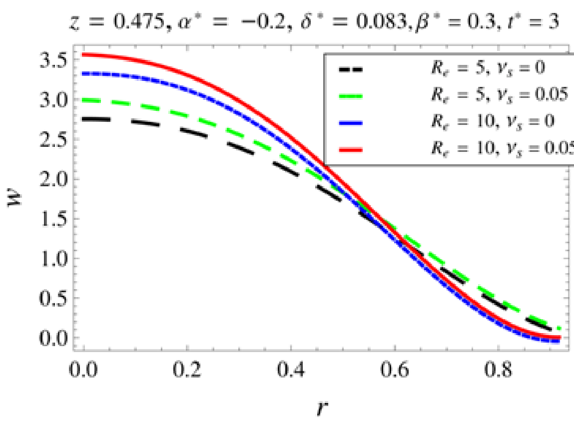

Figure 4 Outcomes of R_e on velocity profile for non-Newtonian fluid.

It is depicted from Figure 6 that with and without slip velocity of the fluid expanded with a rise in time, same behavior for Newtonian fluids can be seen from Figure 7. Moreover, it is noted that enhancement in velocity for non-Newtonian fluid is greater than Newtonian fluid due to slip velocity. The effects of Reynolds number on dimensionless pressure gradient between $z = \pm 1$ is shown in (Figure 8) (Figure 9). It is notable that the pressure gradient raises up to the throat of the constriction and then declines in the diverging portion for both non-Newtonian and Newtonian fluids with and without velocity slip. In the meanwhile it is evident from the (Figure 8) (Figure 9) that the pressure gradient contracted with rise in Reynolds number.

Effects of non-Newtonian parameters on pressure gradient is given in (Figure 10) (Figure 11)that the pressure rises as non-Newtonian parameters boost and the slip velocity declines the pressure gradient.

Same conduct for constriction height δ^* on the pressure gradient is observed in (Figure 12) (Figure 13). (Figure 14) (Figure 15)presents the effect of deviation of time on pressure gradient for non-Newtonian and Newtonian fluids. The results found for Newtonian fluids are same as discussed by DF Young.[10]

The analytical distribution of shearing stress along the wall is shown in Figures 16−20.

It is observed from the (Figure 16) (Figure 17)that for any Reynolds number, the shearing stress attains a large value on the throat and then promptly declines in the diverging section. It is notable here that shear stress declines with a rise in Reynolds number and slip velocity decreases the wall shear stress. It means that Reynolds number and slip velocity provide a mechanism to control the wall shear stress. Figure 18 shows that as non-Newtonian parameter β^* expanded wall shear stress also rises, which was expected naturally.

(Figure 19) (Figure 20)shows that wall shear stress increases with an increase in time t^* and decreases with slip velocity.

(Figure 21) (Figure 22) shows the effects of constriction on the separation and reattachment points respectively. It is noted, as naturally expected, that separation point intricate with a rise in non-Newtonian parameter β^* while reattachment point downward.

It is notable here that the separation point intricate and the reattachment point moves downward with velocity slip v_s .

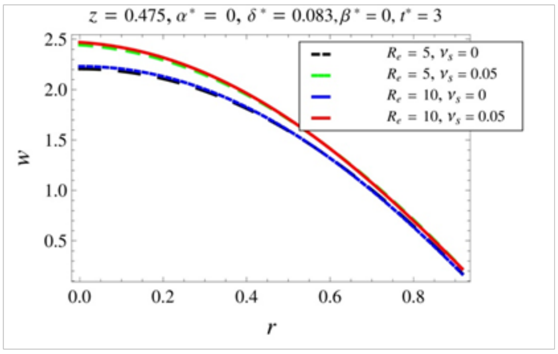

Figure 5 Effect of R_e on velocity profile for Newtonian fluid.

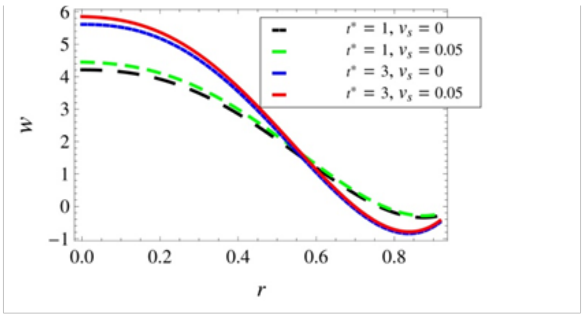

Figure 6 Outcomes of time t^* on velocity profile for non-Newtonian fluid.

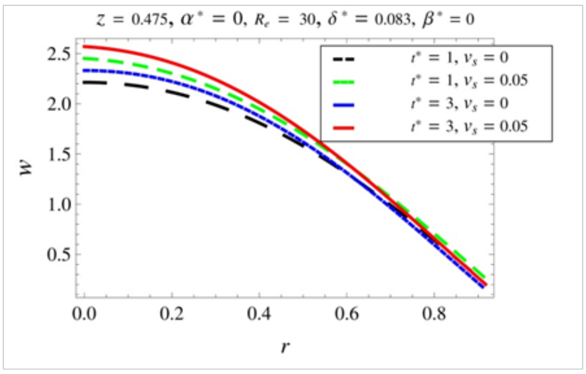

Figure 7 Effect of t^* on velocity profile for Newtonian fluid.

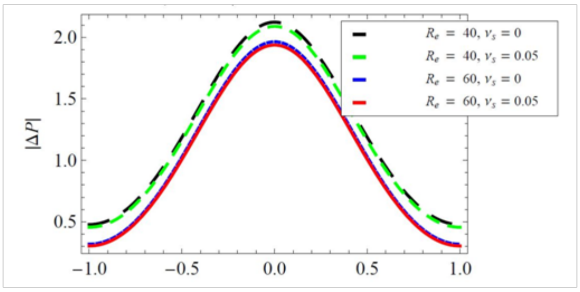

Figure 8 Effect of R_e on pressure gradient for non-Newtonian fluid.

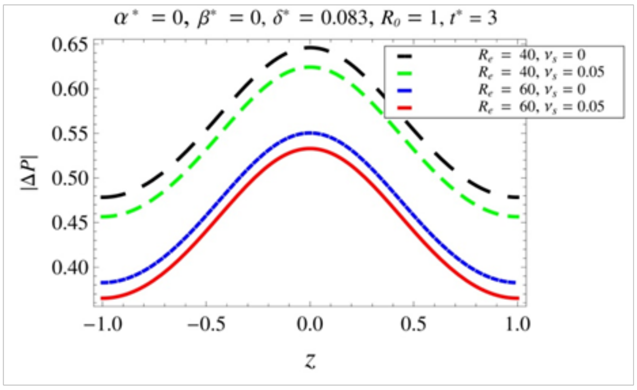

Figure 9 Effect of R_e on pressure gradient for Newtonian fluid.

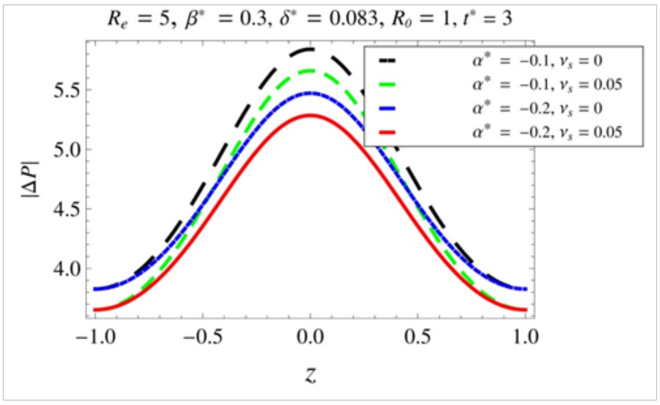

Figure 10 Effect of non-Newtonian parameter α^* on pressure gradient.

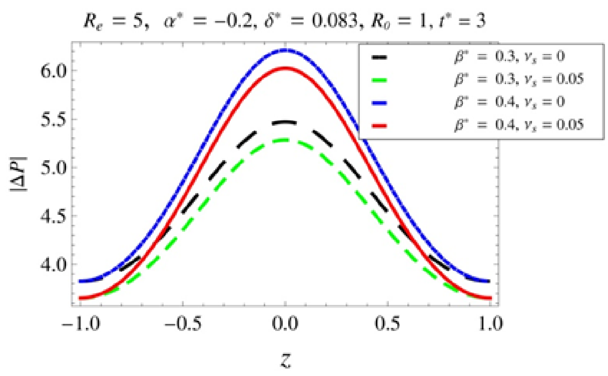

Figure 11 Effect of non-Newtonian parameter β^* on pressure gradient.

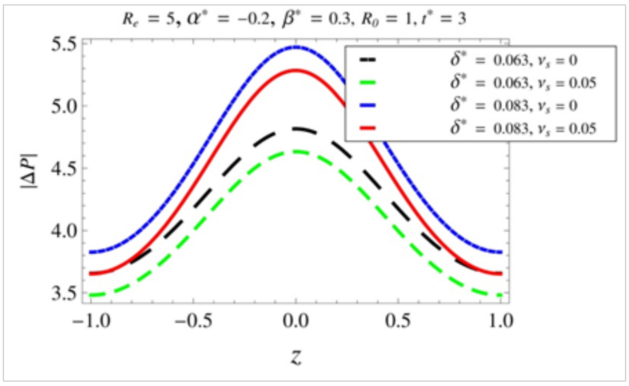

Figure 12 Effect of δ^* on pressure gradient for non-Newtonian fluid.

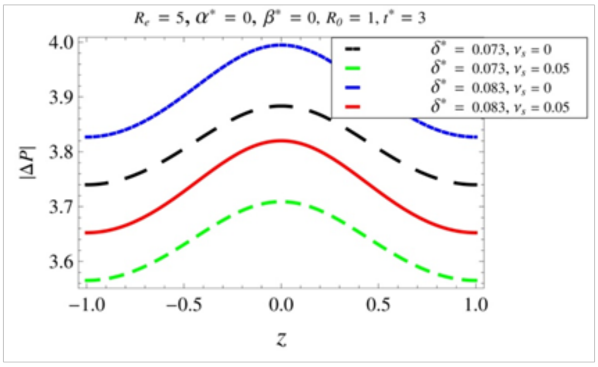

Figure 13 Effect δ^* on pressure gradient for Newtonian fluid.

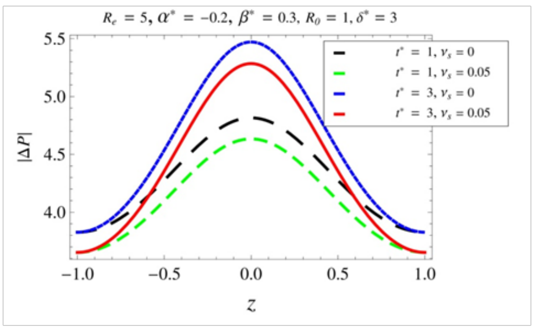

Figure 14 Effect of t^* on pressure gradient for non-Newtonian fluid.

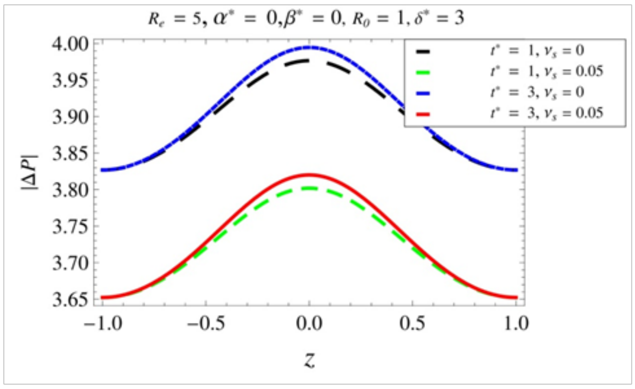

Figure 15 Effect t^* on pressure gradient for Newtonian fluid.

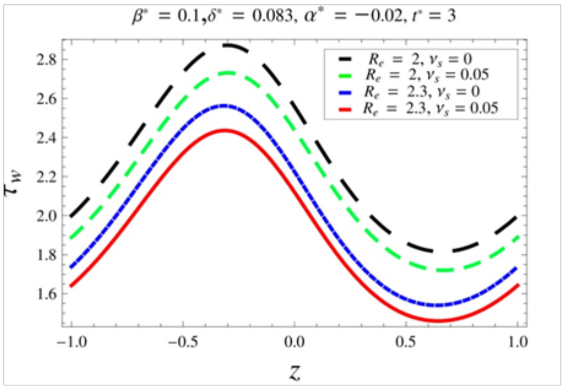

Figure 16 Effect of R_e on shear stress for non-Newtonian fluid.

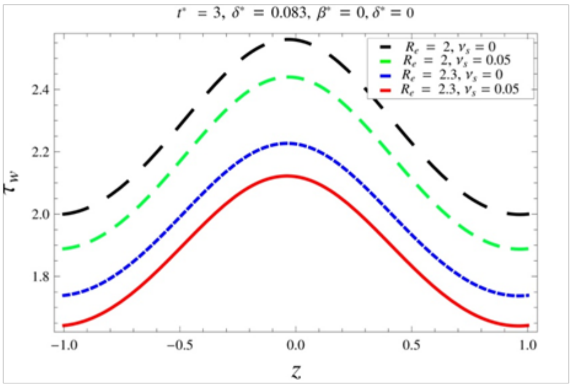

Figure 17 Effect of R_e on shear stress for Newtonian fluid.

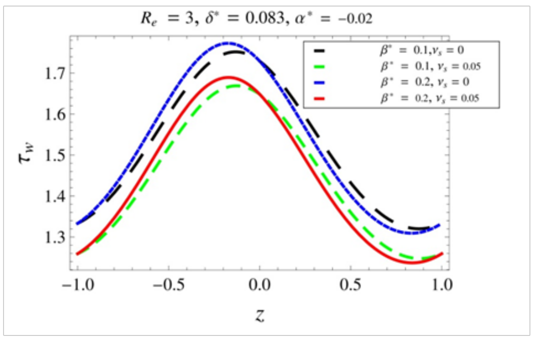

Figure 18 Effect of β^* on wall shear stress.

Citation: Khan NZ, Rana MA, Siddiqui AM. Effect of a time dependent stenosis on flow of a second order fluid through constricted tube with velocity slip at wall using integral method. *Fluid Mech Res Int.* 2018;2(3):118–126. DOI: 10.15406/fmrij.2018.02.00027

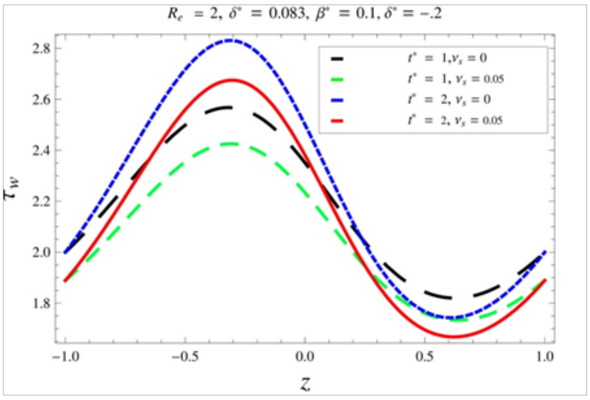

Figure 19 Effect of on shear stress for non-Newtonian fluid.

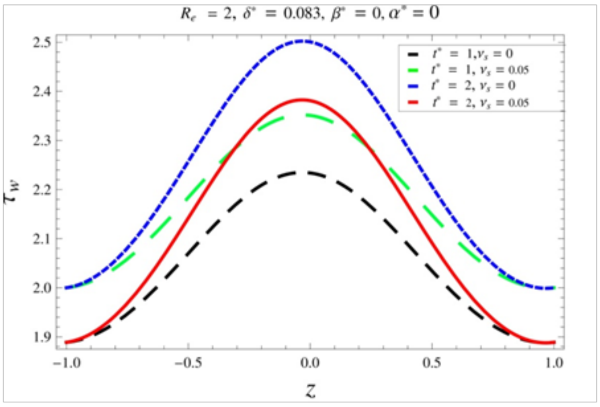

Figure 20 Effect of on wall shear stress for Newtonian fluid.

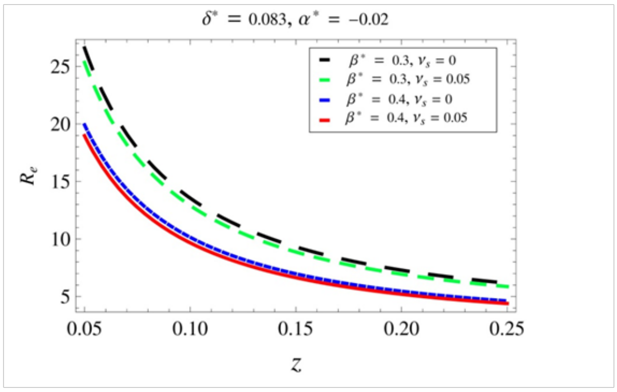

Figure 21 Separation points for non-Newtonian parameter β^*.

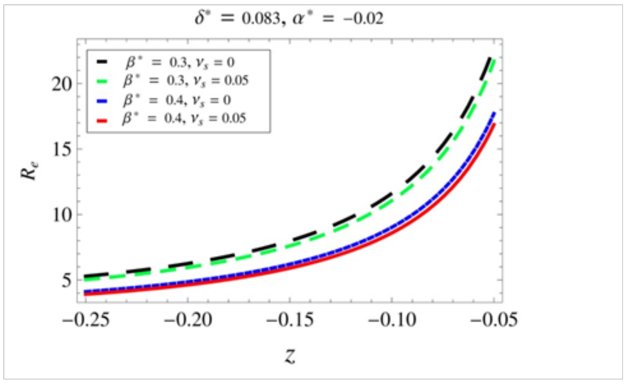

Figure 22 Reattachment points for non-Newtonian parameter β^*.

Conclusion

In this work an incompressible, steady and laminar flow of a second order fluid through time dependent obstructed tube is modeled and analyzed theoretically. The fluid is taken as blood flowing through the artery and the results are pertinent to mild stenosis. The characteristics of fluid such velocity field, pressure gradient, wall shear stress and separation phenomena for the geometry of the time dependent constriction are presented. An integral momentum method is applied for the solution of the problem. In human body blood flow is laminar so the Reynolds number taken in the present theoretical study is very close to natural phenomena.[5,38] Usually the slip velocity is taken as the 10 percent of the average velocity.[30,39] Therefore we have followed this approach. The present study can be summarized as below:

As non-Newtonian parameter increases velocity increases.

1. Viscous forces are dement over inertia forces near the throat of the constriction, however, opposite results is observed in the diverging portion.
2. Reynolds number and non-Newtonian are the parameter to controls the wall shear stress.
3. The separation and reattachment points vary with Reynolds number.
4. Slip velocity has increasing effects on velocity profile while decreasing on pressure gradient and wall shearing stress.

The present study recovers the theoretical and experimental results for the velocity profile, pressure gradient and wall shear stress of (10) as a major case for $\alpha^* = 0$, $\beta^* = 0$.

variation of time t shows the constriction development

Acknowledgements

None.

Conflict of interest

Author declares there is no conflict of interest in publishing the article.

References

1. DF Young. Fluid Mechanics of arterial stenosis. *Journal of biomechanical engineering*. 1979;101(3):157–75.
2. CG Caro. *Transport of material between blood and wall in arteries.* In Atherogenesis: Initiating factors. Ciba Foundation Medica, Amesterdam: Netherlands; 1973. 127–64 p.
3. DL Fry. *Responses of the Arterial wall to certain physical factors.* In: Atherogenesis: initiating factors. Ciba Foundation Sympozium: Netherlands; 1973. 93–125 p.
4. DF Young, FY Tsai. Flow characteristics in models of arterial stenosis–I-Steady flow. *Journal of Biomechanics*. 1973;6(4):395–411.
5. JH Forrester, DF Young. Hemodynamic factors in Atherogenesis cardiovascular diseases. In: Scheiberg, editors. Raven Press: New York; 1976. 77–95 p.

6. L Dintenfass. Viscosity factors in hypertensive and cardiovascular disease. *Cardiovascular Med*. 1977;2:337−363.
7. S Chien. Hemorheology in clinical medicine: Recent Advances in cardiovascular disease. In: Niimi H, editor. Suita, Osaka, Japan; 1981. p. 21−6.
8. CG Caro. *Arterial fluid mechanics and Atherogenesis: Hemorheological Approach to Cardiovascular Diseases*. In: Hideyuki Niimi, Takehiko Azuma, Yukihide Isogai editors. Proceedings of the Satellite Meeting of the IV International Congress of Biorheology. Osaka, Japan. 1981.
9. H Schmidt Schonbein. *Fluidity of blood in microvessels: consequences of red cell behaviour and vasomotor activity.* 4th International conference of Biorheology, Jikei University, Japan. 1981. p. 20.
10. DF Young. Effect of a time dependent stenosis on flow through a tube. *Journal of Engineering for Industry*. 1968;90(2):248−254.
11. BE Morgan, DF Young. An integral method for the analysis of flow in arterial stenosis. *Bulletin of Math Bio.* 1974;36:39−53.
12. MD Deshpande, DP Gidden, RF Mabon. Steady laminar flow through modelled vascular stenosis. *Journal of Boimechanics*. 1976;9(4):165−74.
13. DA MacDonald. On steady flow through modelled vascular stenosis. *Journal of Biomechanics*. 1979;12(1):13−20.
14. JB Shukla, RS Parikar, SP Gupta. Effects of perpheral layer viscosity on blood flow through the artery with mild stenosis. *Bulliten of Mathematical Biology*. 1980;42(6):797−805.
15. J Perkkio, R Keskinen. On the effect of the concentration profiles of red cells on blood flow in the artery with stenosis. *Bull Math Biol.* 1983;45(2):259−67.
16. JB Shukla, RS Parikar, BP Rao. Effects of stenosis on non−Newtonian flow of blood in an artery. *Bulliten of Mathematical Biology*. 1980;42(3):283−94.
17. SA Ahmed, DP Gidden. Velocity measurement in steady flow through Axisymmetric stenosis at moderate Reynolds number. *J Biomech*. 1983;16(7):505−516.
18. DF Young, FY Tsai. Flow characteristics in models of arterial stenosis−II. Unsteady flow. *J Biomech*. 1973;6(5):547−59.
19. EW Merill. Rheology of human blood and some speculations on its role in vascular homeostasis: *Biomechanical mechanisms in vascular homeostasis and intravascular thrombosis*. In: PN Sawyer, editor. New York, Appleton century-crofts; 1965. p. 121−137.
20. D Biswas. *Blood flow models: A comparative study.* India: Mittal Publications; 2000. p.103−120.
21. SR Verma. Analytical study of blood flow through an artery with mild stenosis. *Acta Ciencia Indica*. 2009;2:281.
22. A Mirza, A Ansari, AM Siddiqui, et al. On steady two-dimensional flow with heat transfer in the presence of a stenosis. *WEAS Transactions on fluids mechanics*. 2013;8(4):149−158.
23. AM Siddiqui, NZ Khan, MA Rana. et al. Flow of a second grade fluid through constricted tube using integral method. *Journal of Applied Fluid Mechanics*. 2016;9(6):2803−12.
24. L Benet. Red cell slip at wall *in vitro*. *Science*. 1967;155(3769):1554−6.
25. G Bugliarello, JW Hyden. High speed microcinematograhic studies of blood flow *in vitro*. *Science*. 1962;138(3544):981−3.
26. Y Nubar. Blood flow, slip and viscometry. *Biophysical Journal*. 1971;11(3):252−264.
27. V Vand. Viscosity of solutions and suspensions. *J Phys Chem*. 1948;52(2):277−99.
28. I Isenberg. A note on the flow of blood in cappillary tubes. *The bulletin of mathematical biophysics*. 1952;15(2):148−152.
29. P Brunn. The velocity slip of polar fluids. *Rheologica Acta*. 1975;14(12):1039−54.
30. JC Misra, BK Kar. Momentum Integral method for studying flow characteristics of blood through a stenosed vessel. *Biorheology*. 1989;26(1):23−35.
31. JC Misra, GC Shit. Rloe of slip velocity in blood flow through stenosed arteries: A non-Newtonian model. *J Mech Med Biol*. 2007;7(3):337−353.
32. MD Shamshuddin, OA Beg, RM Sunder, et al. Finite element computation of multi-physical micropolar transport phenomena from an inclined moving plate in porous media. *Indian Journal of Physics*. 2018;92(2):215−30.
33. MD Shamshuddin, SR Misra, OA Beg, et al. Unsteady reactive radiative micropolar flow, heat and mass transfer from an inclined plate with Joule heating: A model for electro-conductive polymer processing. *Part C: Journal of Mechanical Engineering Science*. 2018.
34. MD Shamshuddin, SS Reddy, Beg OA, et al. Rotating unsteady multi-physico-chemical magneto-micropolar transport in porous media: Galerkin finite element study. *Computational Thermal Sciences*. 2018;10(2):167−97.
35. SU Siddiqui, SR Shah, Geeta. A biomechanical approach to study the effect of body acceleration and slip velocity through stenotic artery. *Applied Mathematics and Computation*. 2015;261:148−55.
36. A Bhatnagar, RK Shivastav, AK Singh. Effect of slip velocity on blood flow through composite stenosed Arteries: A Herschel-Bulkely fluid model. *National Academy of Science Letter*. 2015;38(3):251−55.
37. NZ khan, AM Siddiqui, MA Rana. Flow of a second order fluid through constricted tube using integral method. *International Journal of Mathematical, Computational, Physical, Electrical and Computer Engineering*. 2015;9(10):636−42.
38. JH Forrester, DF Young. Flow through a converging−diverging tube and its implications in occlusive disease. *Journal of Biomechanics*. 1970;3:297−316.
39. PN Tandon, VK Ktiyar. Flow through a tube with time dependent stensis. *Medical and Life Science Engineering*. 1976;2:39−47.
40. TC Papanastasiou, GC Georgiou, AN Alexandrou. *Viscous Fluid Flow*. USA: CRC press; 1999. p. 69−72.
41. BD Coleman, W Noll. An approximate theorem for functionals, with appliications in continuum mechanics. *Archives of Rational Mechanics and Analysis*. 1960;6(1):355−70.
42. H Schlichting. *Boundary Layer Theory*. 6th ed New York: McGraw Hill; 1968. p. 122−92.
43. JH Forrester, DF Young. Flow through a converging−diverging tube and its implications in occlusive disease. *J Biomech*. 1970;(3):297−316.
44. SR Verma. *Study of blood flow through modelled vascular stenosis.* DAV College Kanpur: India; 2012. p. 1−21.